Fuel-Optimal Collision-Free Trajectory Planning of Low-Earth Orbit Satellites under Modeling Uncertainties and Orbital Perturbations

Himadri Basu *, Yasaman Pedari †, Mads Almassalkhi ‡, Hamid R. Ossareh §
University of Vermont, Burlington, VT 05405, USA.

In this paper, we present a collision-free fuel-optimal trajectory optimization (TO) problem for large-scale satellite swarm reconfiguration in a circular low earth orbit (LEO) under perturbations and modeling uncertainties. Non-spherical gravity (J2) of the earth and air drag are two dominant perturbing forces in LEO which causes significant orbital measurement errors and eventually sub-optimal actuation and trajectory prediction by TO. By quantifying the modeling uncertainties and errors associated with various relative dynamical models of satellites, we identify a suitable model for the TO algorithm. To address the computational challenges associated with the final configuration of satellites on the target formation, we first decouple the assignment problem from TO and evaluate the fuel costs for each satellite to reach to each of the target locations on the final formation. By using this fuel cost information, we then derive fuel optimal final configuration and trajectories of satellites. To make these satellite trajectories maintain inter-satellite safety distance at all times, we propose two approaches: 1) distributed approach where collision avoidance (CA) constraints are considered to be part of the path planning algorithm and all the satellites cooperatively find collision free feasible paths with least fuel consumption, and 2) centralized approach where CA constraints are directly included into the final configuration assignment problem, which allows to derive final configuration and corresponding satellite trajectories that maintain inter-satellite safety distance. With the help of numerical examples, we illustrate the performance, computation time complexity and fuel optimality of both approaches with increasing swarm size and safety distance. Finally, to mitigate the effects of modeling uncertainties, unmodeled perturbations and sampling errors in predicted satellite trajectories, we present shrinking horizon model predictive control (SHMPC) that updates the future control commands based on new state information from the actual satellite motion.

*Postdoctoral Associate, Department of Electrical and Biomedical Engineering, himadri.basu@uvm.edu
†Graduate Research Assistant, Department of Electrical and Biomedical Engineering, yasaman.pedari@uvm.edu
‡Associate Professor, Department of Electrical and Biomedical Engineering, malmassa@uvm.edu
§Assistant Professor, Department of Electrical and Biomedical Engineering, hossareh@uvm.edu

Nomenclature

R_e	=	6378km, earth's mean equatorial radius
J_2	=	1.082×10^{-3}, second zonal harmonic constant
K_{J2}	=	$1.5\mu J_2 R_e^2 = 2.633 \times 10^{10}$ km^2 s^{-2}
μ	=	398600 km s^{-2}
N	=	number of spacecrafts
$\mathcal{N}_j$	=	neighborhood set of satellite j
T	=	one orbital period
R_{safe}	=	minimum inter-satellite distance to avoid collision risk
R_{comm}	=	communication distance between two neighboring spacecrafts
a	=	semimajor axis
e	=	eccentricity
h	=	angular momentum
i	=	inclination angle
Ω	=	right ascension of the ascending node (RAAN)
θ	=	geodesic latitude
(X, Y, Z)	=	Earth-centered inertial (ECI) coordinate system
r	=	orbital position in ECI coordinates
v_x	=	orbital velocity in ECI coordinates
(x, y, z)	=	unit vectors of local-vertical/local-horizontal coordinate frame
$\bar{\boldsymbol{r}}_j$	=	$\begin{bmatrix} x_j & y_j & z_j \end{bmatrix}^{\mathrm{T}}$ is relative position vector of j^{th} satellite in LVLH frame
$\dot{\bar{\boldsymbol{r}}}_j$	=	$\begin{bmatrix} \dot{x}_j & \dot{y}_j & \dot{z}_j \end{bmatrix}^{\mathrm{T}}$ is relative velocity vector of j^{th} satellite in LVLH frame
$(\omega_x, \omega_y, \omega_z$	=	angular velocity velocity in LVLH frame
$(\alpha_x, \alpha_y, \alpha_z)$	=	linear acceleration vector of j^{th} satellite in LVLH frame
(a_{jx}, a_{jy}, a_{jz})	=	angular acceleration vector of j^{th} satellite in LVLH frame
$\boldsymbol{V}_a$	=	orbital velocity vector relative to atmospheric drag
ω_e	=	7.9921×10^{-5} rad s^{-1}
$\boldsymbol{V}_{aj}$	=	relative velocity vector of j^{th} satellite relative to atmospheric drag
C_d	=	air drag coefficient
A/m	=	cross-section of spacecraft per unit mass
ρ	=	air density
t_f	=	terminal time of the optimization problem

k = sampling step size

N_k = terminal time step

u_i = $\begin{bmatrix} u_{i1} & u_{i2} & u_{i3} \end{bmatrix}^{\mathrm{T}}$ control vector for i^{th} satellite in LVLH frame

$u_{m,max}$ = maximum allowable actuation magnitude for m^{th} thruster

$u_{m,min}$ = minimum allowable actuation magnitude for m^{th} thruster

$u^r_{m,max}$ = maximum allowable actuation rate for m^{th} thruster

$u^r_{m,min}$ = minimum allowable actuation rate for m^{th} thruster

$u_{\max}$ = $\begin{bmatrix} u_{1,\max} & u_{2,\max} & u_{3,\max} \end{bmatrix}^{\mathrm{T}}$

$u^r_{\max}$ = $\begin{bmatrix} u^r_{1,\max} & u^r_{2,\max} & u^r_{3,\max} \end{bmatrix}^{\mathrm{T}}$

$\boldsymbol{x}_i(k)$ = $\begin{bmatrix} \bar{\boldsymbol{r}}_i(k) & \dot{\bar{\boldsymbol{r}}}_i(k) \end{bmatrix}^{\mathrm{T}}$ is state vector of the optimization problem at time step k for satellite i

$\boldsymbol{x}^{\boldsymbol{m}}_i(k)$ = the solution to optimization problem at $\boldsymbol{m}^{\text{th}}$ iteration

$\bar{\boldsymbol{x}}_i(k)$ = nominal state vector of satellite i used in the optimization problem

$\boldsymbol{x}_{iS}$ = initial state vector of satellite i

$\boldsymbol{x}_{iD}$ = terminal state vector of satellite i

$\boldsymbol{x}_S$ = $\begin{bmatrix} \boldsymbol{x}^{\mathrm{T}}_{1S} & \boldsymbol{x}^{\mathrm{T}}_{2S} & \cdots & \boldsymbol{x}^{\mathrm{T}}_{NS} \end{bmatrix}^{\mathrm{T}}$

$\boldsymbol{x}_D$ = $\begin{bmatrix} \boldsymbol{x}^{\mathrm{T}}_{1D} & \boldsymbol{x}^{\mathrm{T}}_{2D} & \cdots & \boldsymbol{x}^{\mathrm{T}}_{ND} \end{bmatrix}^{\mathrm{T}}$

$d(i,:,q,:)$ = $\min\limits_{\forall k \in \{1,N_k\}} \boldsymbol{x}_i(k) - \boldsymbol{x}_q(k)\|$ minimum inter-satellite distance between i and q

$\|.\|_p$ = l_p norm of a vector, $p \in [1,\infty)$

I_p = identity matrix of order p

0_p = zero vector of dimension $p \times 1$

$O(.)$ = computation time complexity

f_{ij} = fuel cost for satellite i to move to location j in the final formation

F = $[f_{ij}]_{N\times N}$ fuel cost matrix

$d^{\min}_{i,j}$ = minimum distance between location i and j in initial and final formation respectively

Shorthand Notations

s_θ (or c_θ) = $\sin(\theta)$ (or $\cos(\theta)$)

Subscripts

S = initial condition ($t = 0$)

D = final condition ($t = t_f$)

i (or j) = spacecraft i (or j)

Superscripts

m = iteration count of SCP

I. Introduction

In this paper, we study satellite formation flying (SFF) in LEO with potential applications in earth observation based missions, such as distributed imaging of earth's surface, atmospheric sampling, and interferometry. SFF has been a topic of significant research interest in recent years as it offers several benefits compared to a large monolithic spacecraft [1, 2] for the same mission such as reduced mission costs, increased flexibility, reconfigurability and performance. The primary task in an earth-observation based SFF mission [3, 4] is to place multiple satellites into nearby orbits forming a satellite cluster to cooperatively achieve a group objective.

A Traditional SFF mission has two primary trajectory design objectives, namely - 1) formation reconfiguration and 2) formation keeping problem. Formation reconfiguration problem typically requires the fleet of spacecraft to perform a series of complex maneuvers such as moving, reorienting and rotating as they move between initial and final formation pairs [5]. When a satellite formation needs to be modified, it is important to determine optimal maneuvers that require minimal fuel consumption while satisfying some physical and mission specific constraints. On the other hand, the objective of the formation keeping problem is to maintain the existing formation of spacecrafts against any orbital perturbations with minimum fuel consumption. In [6], authors proposed a set of J2 invariant initial position and velocity conditions for each spacecraft in a swarm, based on nonlinear energy matching conditions, which would ensure collision free trajectories under J2 gravity and air drag for up to 100 orbital periods. These J2 invariant orbits, also called parking orbits, are very effective at swarm keeping once the swarm is in a desired formation [7]. However, in this work we primarily study the fuel optimal trajectory planning of satellite swarm from the perspective of formation reconfiguration, where the goal is to develop a fuel and computationally efficient guidance and control algorithm for the reconfiguration of LEO satellite swarm.

Fuel/time-optimal control of spacecraft formation based on linear programming was presented in the works of [5, 8, 9] and with nonlinear programming in [3]. In general, SFF with small formation size has been studied well in the literature. Interested readers, please refer to [10, 11] and references therein. By deriving first order KKT conditions, indirect methods in [12, 13] offer a solution to TO problem considering the nonlinear dynamics of swarms of spacecraft. Direct collocation method on the other hand discretizes the control and state space [3], Legendre Pseudo-spectral method approximates the state space with polynomial approximation [14] and the original problem is thus reduced to a nonlinear program which is solved in a centralized manner. Even with the modern computational capabilities, nonlinear

TO programs are not suitable for large-scale trajectory planning. TO problem for a satellite swarm in majority of these works such as in [3, 14] are formulated as nonlinear programs due to either or both the (1) nonlinear spacecraft dynamics, (2) nonconvex collision avoidance (CA) constraints. In [8, 9], a linear relative dynamical model of the satellites used in the TO problem but that ignores the effects of J2 gravity and air drag, which are the most dominant sources of perturbation [15, 16]. In contrast, this paper presents a computationally efficient, scalable TO framework which devotes due consideration on modeling accuracy of satellites in LEO, capturing the effects of both the J2 perturbation and air drag with sufficient accuracy.

Hill-Clohessy-Wiltshire (HCW) equations are shown to be good linear approximations of the relative dynamics in circular LEO around a perfectly spherical and homogeneous earth [17, 18]. In reality, due to the non-uniform gravitational pull resulted from earth's oblateness, studying J2 dynamic model of satellite relative motion becomes critical for any SFF mission [19]. Furthermore, in LEO, the air resistance is strong enough to produce a drag modifying the semi-major axis and eccentricity over a sufficiently long period of time [20]. There are several relative dynamical models proposed in the literature, *e.g.* [21, 22], under various assumptions and methodologies, which consider either or both of these effects. A high fidelity nonlinear model considering the effects of J2 drift was developed in [23] for a formation keeping problem, which was later extended to include the effects of air drag in [1]. As the model's complexity hampers its application in control designs [19], we present here a comparative analysis of various dynamical models and then by quantifying modeling errors we identify an appropriate model, specific to LEO SFF mission design.

In this work, we revisit four relative dynamical models - namely: (i) high fidelity nonlinear model in [1] that considers both the effects of J2 and air drag, (ii) linearized J2 model in [23], (iii) Hill's equations in [17], (iv) Modified Hill's equations with J2 in [18]. To select an appropriate model for TO, we first compare relative dynamical models (ii)-(iv), stated above, with respect to a high fidelity nonlinear model (i) and compute modeling errors for various initial conditions. This analysis has not been conducted in a cohesive manner before, and modeling errors have not been formally quantified. We fill this gap and quantify the errors, which allows us to identify linearized J2 as an excellent candidate to be used as computationally simple state space constraints in trajectory planning problem.

One of the key challenges in cooperative trajectory planning and control problem for a considerable swarm size is the computational aspects associated with the large information flow and the amount of processing required [8]. Primary difficulties in designing a computationally efficient TO algorithm are caused by (1) the assignment of satellites in a fuel-optimal configuration on the final formation [8] and (2) the nonconvex formulation of CA constraints [3]. Given a set of positions and velocities on a final formation of the satellite swarm, the objective of an assignment problem is to place each satellite to a specific final destination in a way that is fuel optimal for the entire fleet. We present here an alternative approach to decouple the final configuration assignment problem, also called path assignment (PA) problem, from the optimization algorithm to make this more tractable computationally at the expense of negligible loss (at most 2%) in fuel-optimality. In this approach, satellites analyze each of the target locations in the final formation and evaluate

the fuel cost to reach at each of these locations from their respective initial positions by solving decentralized linear programs in parallel [8]. Using this fuel cost associated with each configuration, a mixed-integer linear program (MILP) formulation is proposed, which allows to determine a configuration and the satellite trajectories that are fuel optimal for the entire fleet. This approach alleviates the large communication overhead in the distributed auction based assignment problem proposed in [24].

On the other hand, there are numerous methods in the existing texts to solve trajectory planning problem with CA, which can be broadly classified into three categories, namely - (1) stochastic approach [25], (2) heuristic approach [5] and (3) convex approximations [6, 7, 26]. Mixed-integer linear programming was used in [9] for trajectory planning with CA. However, this approach scales poorly with swarm size due to a large number of binary variables being introduced into the TO formulation. In the works of [26], authors proposed a TO algorithm with heuristic CA constraints which result in a overly conservative approximation of the collision free feasible region. To address these problems, in this work, we offer two novel TO algorithms which differ from one another on how CA constraints are formulated.

In the first approach, we adopt sequential convex programming (SCP) based distributed TO solution to swarm reconfiguration problem in [6] with affine approximation of CA constraints. Given a set of initial and final swarm configuration, obtained as a solution to the assignment problem, TO algorithm with convexified CA constraints in approach 1 allows us to iteratively determine collision-free fuel optimal trajectories. Since in this case, all the participating satellites share in real-time their recent location information with the other neighboring satellites, approach 1 may lead to large communication overhead for a considerable swarm size. To mitigate this, instead of including CA constraints in the TO formulation, in approach 2 we rather determine the configuration that allow the satellites to maintain necessary inter-satellite distance at all times. Therefore, CA constraints are now embedded within the PA problem with an objective to find near optimal final configuration and collision free trajectories. With the help of numerous illustrative examples, we demonstrate the performance, computational advantages and loss of optimality of both approaches.

Another key question that arises for any trajectory generation process, as noted in [8], is the effect of modeling uncertainties and ignored nonlinear effects (e.g., solar radiation pressure). To robustify the trajectory planner against initial states, "multiple-model" approach was proposed in [8]. Uncertainties associated with sensing, actuation, initial states and unmodeled disturbances are addressed in this paper by developing a robust trajectory planning formulation with shrinking horizon model predictive control (SHMPC) that mitigates the accumulation of modeling errors in every prediction horizon. SHMPC can be viewed as a variant of traditional MPC [7, 27], where the prediction horizon shrinks in every iteration unlike MPC. SHMPC computes the control input by optimizing over a finite-horizon subject to control and state constraints with the current state as the initial state of the optimization and terminal state as the fixed final state. Then, the control input is applied to the system until a new computation is completed giving an updated control input.

Contributions: In this work, we present a computationally efficient trajectory planning algorithm of large scale

SFF, which is appropriate for use in implementation of coordination and control architecture in practical missions. Main contributions are (1) quantification of uncertainties around different models, and selection of linearized J2 model as suitable relative state space dynamical system for TO problem, (2) decoupling of assignment algorithm from the TO problem to efficiently compute near-optimal satellite trajectories under given mission specifications, (3) two novel approaches to solve trajectory planning problem with CA constraints, (4) comparative analysis on performance, computational complexity and fuel-optimality, and (5) SHC to iteratively mitigate the effects of any modeling uncertainties and sampling errors.

The organization of the paper is as follows. In Section II, we review some preliminaries of swarm reconfiguration problem, present the problem statement along with the mission specifications. In Section III, we review various relative dynamical models of satellites, evaluate modeling errors and consequently quantify uncertainties in Section IV. Next, we formulate our TO problem with PA and CA constraints in Section V along with our proposed approaches to decouple the problem in various subcomponents. To robustify against modeling uncertainities and perturbations, we introduce the structure of SHMPC algorithm to be used in subsequent sections. In Section VI and VII, we present two novel approaches to solve TO problem with CA constraints along with suitable numerical examples. We compare the performance, computation time complexity and fuel optimality of these approaches in Section VIII. Finally, some concluding remarks and future research directions are given in Section IX.

II. Problem Statement

In this section, we review the preliminaries of swarm reconfiguration problem and define the problem objective. Given initial and final formation of N identical satellites in close proximity in circular LEO subject to J2 gravity and air drag, the objective of this paper is to derive a computationally efficient, scalable TO framework satisfying all physical and mission specific constraints, discussed below, such that all these satellites under predicted actuation from the trajectory planning algorithm, make optimal maneuvers to reach to the final formation after a specified time duration with minimal fuel consumption. The results presented here are relevant for practical space missions related to SAR interferometry, imaging of earth's surface, etc.. Inspired by the interferometry missions [6, 26], we specifically focus on swarm reconfiguration problem that involves transfer of hundreds of satellites from one J2 invariant passive circular orbits (PCO) to the other with minimum fuel consumption while avoiding any inter-satellite collisions. In the works of [6, 7], J2 invariant PCOs have been found to provide collision free navigation for large satellite swarm (≈ 500) for more than 100 orbital periods and thus serves as an excellent configuration for swarm keeping.

In the traditional texts on dynamical motion of satellites, an unactuated satellite or a fictitious moving point is usually taken as a reference and other participating satellites in formation as followers. Given the initial orbital elements, the position and velocity vectors of this reference satellite at every time instant define a target orbit. This target orbit is generally expressed in Earth-centered inertial (ECI) coordinate frame which has its origin located at the center of the

earth, X axis aligned with earth's mean equator and passes through vernal equinox, Z axis along the celestial north pole while the Y axis completing the right hand orthogonal frame with the other two [18].

The relative dynamical motion of all follower satellites on the other hand are described in local-vertical-local-horizontal (LVLH) frame [28], with its origin located on the target orbit. In this local coordinate frame, the relative position vector of j^{th} spacecraft is usually expressed as $\bar{\mathbf{r}}_j = \begin{bmatrix} x_j & y_j & z_j \end{bmatrix}^{\mathrm{T}}$ where the unit vectors associated with x_j, y_j and z_j respectively point in the radial, along-track and across-track directions. LVLH frame is a rotating coordinate frame which rotates at ω_x rad s^{-1} in radial direction and ω_z rad s^{-1} in across-track direction. The relative motion of satellites in LVLH frame serves as a state-space constraint in the TO problem.

A. Nonlinear relative motion of satellites

A high-fidelity nonlinear relative motion of satellites was presented in [1] considering the effects of both J2 and air drag. As described in [1], the equations of motion for j^{th} spacecraft under J2 perturbation and atmospheric drag, relative to the target orbit are given as follows.

$$\ddot{x}_j = 2\dot{y}_j\omega_z - x_j(n_j^2 - \omega_z^2) + y_j\alpha_z - z_j\omega_x\omega_z + a_{jx} - \bar{\zeta}\mathrm{s}_i\mathrm{s}_\theta - r(n_j^2 - n^2) - l_{1j}(\dot{x}_j - y_j\omega_z) - l_{2j}v_x, \tag{1}$$

$$\ddot{y}_j = -2\dot{x}_j\omega_z + 2\dot{z}_j\omega_x - x_j\alpha_z - y_j(n_j^2 - \omega_z^2 - \omega_x^2) + z_j\alpha_x - \bar{\zeta}\mathrm{s}_i\mathrm{c}_\theta + a_{jy}, \tag{2}$$

$$\ddot{z}_j = -2\dot{y}_j\omega_x - x_j\omega_x\omega_z - y_j\alpha_x - z_j(n_j^2 - \omega_x^2) - \bar{\zeta}\mathrm{c}_i + a_{jz}, \tag{3}$$

where $l_{1j} = C\|\mathbf{V}_{aj}\|, l_{2j} = C(\|\mathbf{V}_{aj}\| - \|\mathbf{V}_a\|), \bar{\zeta} = \zeta_j - \zeta$ with

$$\begin{aligned}
\zeta &= \frac{2K_{J2}\mathrm{s}_i\mathrm{s}_\theta}{r^4}, \zeta_j = \frac{2K_{J2}r_{jZ}}{r^5},\ n^2 = \frac{\mu}{r^3} + \frac{K_{J2}}{r^5} - \frac{5K_{J2}\mathrm{s}_i^2\mathrm{s}_\theta^2}{r^5},\\
n_j^2 &= \frac{\mu}{r_j^3} + \frac{K_{J2}}{r_j^5} - \frac{5K_{J2}r_{jZ}^2}{r_j^7},\ r_j = \sqrt{(r + x_j)^2 + y_j^2 + z_j^2},\\
r_{jZ} &= (r + x_j)\mathrm{s}_i\mathrm{s}_\theta + y_j\mathrm{s}_i\mathrm{c}_\theta + z_j\mathrm{c}_i,\ \alpha_z = -\frac{2hv_x}{r^3} - \frac{K_{J2}}{r^5}\mathrm{s}_i^2\mathrm{s}_{2\theta},\\
\alpha_x &= f_x - \frac{K_{J2}\mathrm{s}_{2i}\mathrm{c}_\theta}{r^5} + \frac{3v_xK_{J2}\mathrm{s}_{2i}\mathrm{s}_\theta}{r^4h} - \frac{8K_{J2}^2\mathrm{s}_i^3\mathrm{c}_i\mathrm{s}_\theta^2\mathrm{c}_\theta}{r^6h^2},\\
f_x &= -C\|\mathbf{V}_a\|\omega_e\left(\frac{2rv_x\mathrm{c}_\theta\mathrm{s}_i}{h} - \left(\frac{r}{h}\right)^2\mathrm{c}_\theta\mathrm{s}_i\dot{h} + g_x\right),\ g_x = -\frac{r^2\mathrm{s}_\theta\mathrm{s}_i\dot{\theta}}{h} + \frac{r^2\mathrm{c}_\theta\mathrm{c}_i\dot{i}}{h}
\end{aligned} \tag{4}$$

with $\dot{h}$, $\dot{i}$ and $\dot{\theta}$ are target orbital parameters, given next.

B. Nonlinear target orbit dynamics

Considering the two main disturbances, namely J2 and atmospheric drag, the differential equations governing the motion [1] of the target orbit are

$$\dot{r} = v_x, \tag{5}$$

$$\dot{v}_x = -\frac{\mu}{r^2} + \frac{h^2}{r^3} - \frac{K_{J2}}{r^4}(1 - 3\mathrm{s}_i^2\mathrm{s}_\theta^2) - C\|\mathbf{V}_a\|v_x, \tag{6}$$

$$\dot{h} = -\frac{K_{J2}}{r^3}\mathrm{s}_i^2\mathrm{s}_{2\theta} - C\|\mathbf{V}_a\|(h - \omega_e r^2 \mathrm{c}_i), \tag{7}$$

$$\dot{\Omega} = -\frac{2K_{J2}}{hr^3}\mathrm{c}_i\mathrm{s}_\theta^2 - \frac{C\|\mathbf{V}_a\|\omega_e r^2 \mathrm{s}_{2\theta}}{2h}, \tag{8}$$

$$\dot{i} = -\frac{K_{J2}}{2hr^3}\mathrm{s}_{2i}\mathrm{s}_{2\theta} - \frac{C\|\mathbf{V}_a\|\omega_e r^2 \mathrm{s}_i \mathrm{c}_\theta^2}{h}, \tag{9}$$

$$\dot{\theta} = \frac{h}{r^2} + \frac{2K_{J2}\,\mathrm{c}_i^2\mathrm{s}_\theta^2}{hr^3} + \frac{C\|\mathbf{V}_a\|\omega_e r^2 \mathrm{c}_i \mathrm{s}_{2\theta}}{2h}, \tag{10}$$

$$\mathbf{V}_a = \begin{bmatrix} v_x & (\frac{h}{r} - \omega_e r \mathrm{c}_i) & \omega_e r \mathrm{c}_\theta \mathrm{s}_i \end{bmatrix}^{\mathrm{T}}. \tag{11}$$

For a large-scale satellite swarm with simple onboard computer, the central question to address is how can we make our TO, control and estimation algorithms more computationally efficient so that it meets all the required processing and communication requirements. However, as noted earlier, nonlinear relative motion of satellites, described in (1) – (3), turn the TO into a nonlinear program, which is not computationally feasible for a considerable swarm size with modern optimization solvers such as IPOPT. Therefore, it is necessary to find an appropriate linear dynamical model which captures the effects of perturbing forces and can be used as a suitable alternative for TO problem. To do that, we first revisit various linear dynamical models of satellites in the upcoming section.

Mission specifications : We now summarize below the mission specifications for illustrative numerical simulations presented in this paper. Inspired by a formation flying space mission TechSat-21 [29] by U.S. Air Force Research Laboratory (AFRL) in 2006 and their mission specifications, the position tolerance of the desired relative states in this work are chosen to be 5 m in radial, along-track and across-track directions with respect to the target orbit. For swarm reconfiguration problem with applications in distributed imaging of earth's surface [26], we consider that both the initial and the final formations, centered at the target low earth sun-synchronous orbit (SSO), are concentric PCOs with satellites maintaining at least 50 m safety distance from each other. Additionally, we assume that the initial target orbit is circular and all the satellites are initially located within 15 km from this target orbit. Each satellite is equipped with three thrusters of 3 mN actuation limits with each pointing respectively in radial, along-track and across-track direction. The robust optimal actuation force, as predicted by the TP here is applicable to other thruster configurations as well, namely- coupling thrusters and reaction wheels/magnetometers through a lower-level transformation controller. The results presented here can be directly adopted for practical SFF missions with a swarm size in the order of hundreds.

III. Review of Various Relative Dynamical Models of Satellites

In this section, we review three linear relative dynamical models of LEO satellites, capturing primarily the effects of J2 perturbation.

A. Linearized J2 model

In the high fidelity nonlinear model (1) – (4), there are nonlinear terms n_j^2, ζ_j which include polynomials of the reciprocal of r_j and consequently x_j, y_j, z_j. By using Gegenbauer polynomials, the terms n_j^2 and ζ_j were shown to bear a linear relationship in [23] with the decision variables x_j, y_j and z_j as follows

$$\zeta_j = \zeta - \frac{8K_{J2}x_j \mathrm{s}_i \mathrm{s}_\theta}{r^5} + \frac{2K_{J2}y_j \mathrm{s}_i \mathrm{c}_\theta}{r^5} + \frac{2K_{J2}z_j \mathrm{c}_i}{r^5},$$
$$n_j^2 = n^2 - \frac{3\mu x_j}{r^4} - \frac{5K_{J2}}{r^6}\left[x_j(1-5\mathrm{s}_i^2\mathrm{s}_\theta^2) + y_j\mathrm{s}_i^2\mathrm{s}_{2\theta} + z_j\mathrm{s}_{2i}\mathrm{s}_\theta\right].$$

With the above substitution, the first order linear J2 model yields the following time-varying dynamics

$$\ddot{x}_j = \frac{2\dot{y}h}{r^2} + x_j\left(\frac{2\mu}{r^3} + \frac{h^2}{r^4} + \frac{4K_{J2}(1-3\mathrm{s}_i^2\mathrm{s}_\theta^2)}{r^5}\right) + a_{jx} - y_j\left(\frac{2v_x h}{r^3} - \frac{3K_{J2}\mathrm{s}_i^2\mathrm{s}_{2\theta}}{r^5}\right) + \frac{5K_{J2}\mathrm{s}_{2i}\mathrm{s}_\theta}{r^5}, \tag{12}$$

$$\ddot{y}_j = -\frac{2\dot{x}_j h}{r^2} - \frac{2K_{J2}\dot{z}_j\mathrm{s}_{2i}\mathrm{s}_\theta}{r^3 h} + x_j\left(\frac{2v_x h}{r^3} + \frac{5K_{J2}\mathrm{s}_i^2\mathrm{s}_{2\theta}}{r^5}\right) - y_j\left(\frac{\mu}{r^3} - \frac{h^2}{r^4} + \frac{K_{J2}(1+2\mathrm{s}_i^2 - 7\mathrm{s}_i^2\mathrm{s}_\theta^2)}{r^5}\right)$$
$$+ z_j\left(\frac{3K_{J2}v_x\mathrm{s}_{2i}\mathrm{s}_\theta}{r^4 h} - \frac{2K_{J2}\mathrm{s}_{2i}\mathrm{c}_\theta}{r^5}\right) + a_{jy}, \tag{13}$$

$$\ddot{z}_j = \frac{2K_{J2}\dot{y}_j\mathrm{s}_{2i}\mathrm{s}_\theta}{r^3 h} + \frac{5K_{J2}x_j\mathrm{s}_{2i}\mathrm{s}_\theta}{r^5} - \frac{3K_{J2}y_j v_x \mathrm{s}_{2i}\mathrm{s}_\theta}{r^4 h} - z_j\left(\frac{\mu}{r^3} + \frac{K_{J2}(3-2\mathrm{s}_i^2 - 5\mathrm{s}_i^2\mathrm{s}_\theta^2)}{r^5}\right) + a_{jz}, \tag{14}$$

where r, v_x, h, θ, i are time-varying forcing terms obtained by solving Eqs. (5)–(10).

B. Hill-Clohessy-Wiltshire (HCW) Model with J2

A modified HCW model considering earth's J2 non-spherical effect [18] is given as follows

$$\ddot{x}_j = a_{jx} + 2nc\dot{y}_j + (5k_1^2 - 2)n^2 x_j, \tag{15}$$

$$\ddot{y}_j = a_{jy} - 2nc\dot{x}_j, \tag{16}$$

$$\ddot{z}_j = a_{jz} - k_2^2 z_j, \tag{17}$$

where $k_2 = nk_1 + 1.5J_2\left(\frac{R_e\mathrm{c}_i}{r}\right)^2$, $k_1 = \sqrt{1+k_3}$, $k_3 = 0.375J_2\left(\frac{R_e}{r}\right)^2(1+3\mathrm{c}_{2i})$. In the absence of J2 perturbations, equations (15) – (17) reduce to original HCW model or popularly known as Hill's equation [30].

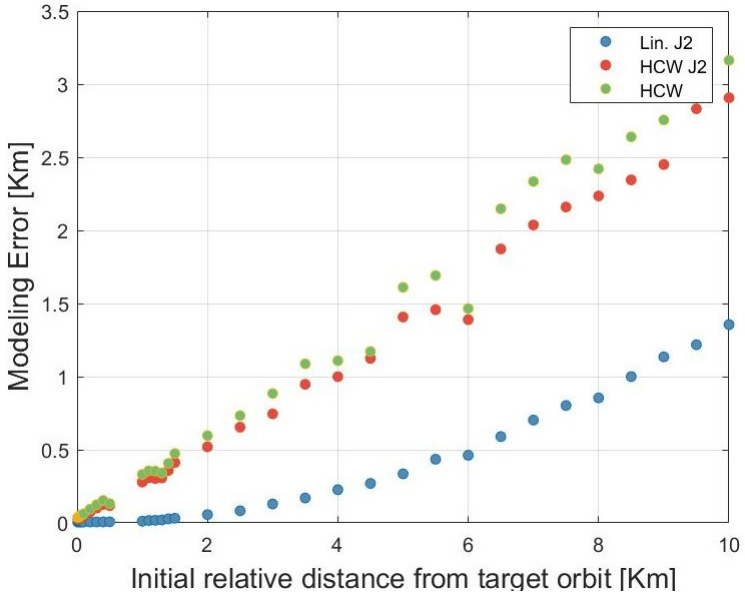

Fig. 1 Maximum modeling error of the three models - Linearized J2, HCW with and without J2 relative to high fidelity nonlinear model (1) **–** (3) **for initial relative distance (LVLH frame)** $[0.01, 10]$ km **and simulation time length** $5T$**.**

IV. Uncertainty Quantification and Modeling Errors

In this section, we compare various dynamical models presented above and evaluate the modeling errors for numerous initial conditions. We are also interested to determine the time instant when the modeling errors go beyond a realistic position tolerance of 5 m [8]. For a given initial condition, we consider a model to be accurate till the time it is within this threshold value. This analysis helps us to determine which model should be used in the TO optimization for a given time window and initial relative position of satellites.

By solving (5)–(10), we obtain the timeseries position, velocity and target orbit elements under J2 perturbation and air drag. With this target orbit data in (12) – (14) and in (15) – (17) we simulate the satellite trajectories in local frame for linearized J2 and HCW model (with and without J2) respectively. For a given initial position and simulation time window, the modeling error of the linearized J2 model is evaluated as the maximum relative distance between the trajectories generated by (12) – (14) and the nonlinear model (1) – (3) for the entire time. Modeling error for HCW with or without J2 are analogously computed with respect to the nonlinear model.

In Fig. 1, we present the maximum modeling errors of the three linear models relative to the high fidelity nonlinear model (1) – (3) under a sinusoidal actuation with frequencies within $[0, 1]$ rad s^{-1}, amplitudes between $[-3, 3]$ mN in a simulation for 5 orbital periods and initial positions drawn randomly from a uniform distribution such that the relative distance for these initial points from the origin lie between $[0.01, 15]$ km. Corresponding to a specific initial distance from the origin in LVLH frame, we randomly pick 150 initial positions, evaluate the maximum of modeling errors for these initial positions and replicate this approach for other initial relative distances and models. From Fig. 1, we observe that the linearized J2 model is more accurate as compared to the other models under considered sinusoidal

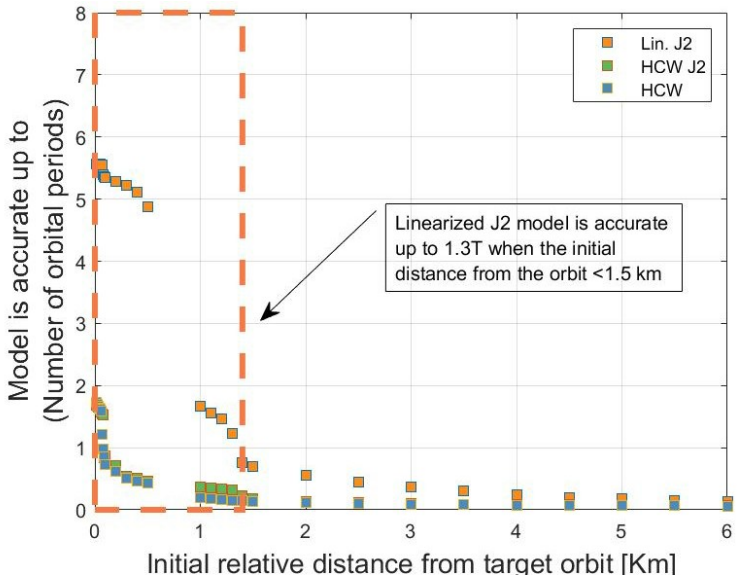

Fig. 2 Accuracy of the three models in terms of the length of time elapsed - linearized J2, HCW with and without J2 for initial relative distance (LVLH frame) $[0.01, 6]$ km**. Corresponding to a specific initial distance, the figure shows the duration until which the trajectory error is smaller than** 5 m **and a model is deemed accurate.**

actuation. We verified this to be true even when there is no actuation.

Next, we evaluate the duration in which all three models yield less than 5 m modeling error under aforementioned sinusoidal actuation. In addition to the modeling errors, we also evaluate the corresponding time instant when this model error exceeds beyond 5 m. The simulation results showing the accuracy of all three models are presented in Fig. 2 from which we observe again that, the linearized J2 model is more accurate than the rest. Precisely, when the initial distance from the target orbit is within 1.5 km, linearized J2 model error is within 5 m for more than one orbital period. Therefore by considering both the modeling error and accuracy time horizon, linearized J2 model is the most appropriate candidate to formulate the relative dynamics of satellite swarms in TO problem with initial distance within 1 km and final time $t_f = 1$ orbital period. For practical mission purposes, where the terminal time is more than one orbital period, we have to restart the TO problem in every one orbital period of time. For convenience, we denote an orbital period of time with T.

V. Formulation of the Basic trajectory planning problem

We present here the TO problem that includes PA, CA constraints in addition to the satellite dynamics and actuation constraints. As noted earlier, for current SFF mission, we specifically focus on moving the satellite swarm from one concentric PCO configuration to another with the center being located on the reference satellite, as shown in Fig. 3. While the unactuated reference satellite moves along a target orbit, other N participating satellites in the swarm make optimal collision-free manuevers to move from one formation to other with the formation center being the reference satellite. Initial and final formations of the swarm reconfiguration problem are given in LVLH frame. The core of this

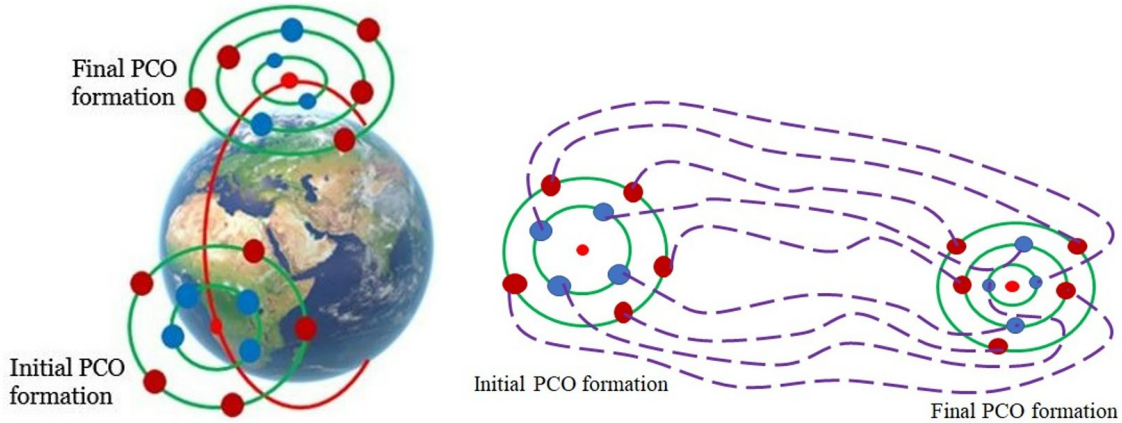

(a) PCO formation reconfiguration of satellite swarm (b) Satellite Paths

Fig. 3 A visualization of swarm reconfiguration problem

optimization problem is to select state variables $\boldsymbol{x}_i(k)$, corresponding control $u_i(k)$ for each spacecraft $i = \{1, 2, \cdots, N\}$ satisfying Euler-discretized version of linearized J2 dynamics (12) – (14) with the form

$$\begin{aligned} &\textbf{state space constraints: } \boldsymbol{x}_i(k+1) = A(k)\boldsymbol{x}_i(k) + Bu_i(k), k = 0, 1, \cdots, N_k - 1 \\ &\textbf{boundary constraints: } \boldsymbol{x}_i(0) = \boldsymbol{x}_{iS}, \boldsymbol{x}_i(N_k) = \boldsymbol{x}_{iD}, \end{aligned} \tag{18}$$

where $\boldsymbol{x}_{iS}$ and $\boldsymbol{x}_{iD}$ are respectively the initial and terminal state vectors for i^{th} spacecraft, and N_k is the terminal time step. Similar to [8, 9], we consider that inputs vectors with their respective slew rates lie within a specified limit

$$\textbf{actuation constraints: } -u_{m,max} \leq u_{im}(k) \leq u_{m,max}, \ m = 1, 2, 3, \tag{19}$$

$$\textbf{slew rate constraints: } u^r_{m,min} \leq u_{im}(k+1) - u_{im}(k) \leq u^r_{m,max}. \tag{20}$$

In contrast to traditional TO problems with well known final configuration [3], we consider that the assignment of the final configuration to each satellite is not known *a priori*. Assignment of final configuration (also called PA problem) is formulated as a mixed-integer linear constraints, given as follows

$$\textbf{PA constraints: } \boldsymbol{x}_i(N_k) = \sum_{j=1}^{N} b_{ij}\boldsymbol{x}_{jD}, \sum_{i=1}^{N} b_{ij} = 1, \sum_{j=1}^{N} b_{ij} = 1, \tag{21}$$

where the unity row sum and column sum of the assignment matrix $\mathcal{B} = \left[b_{ij}\right]_{N\times N}$ ensures that each of these terminal points $\boldsymbol{x}_{iD}$, $i = 1, 2, \cdots, N$ is assigned to only one of the satellites. Furthermore, at all times, during the manuever the

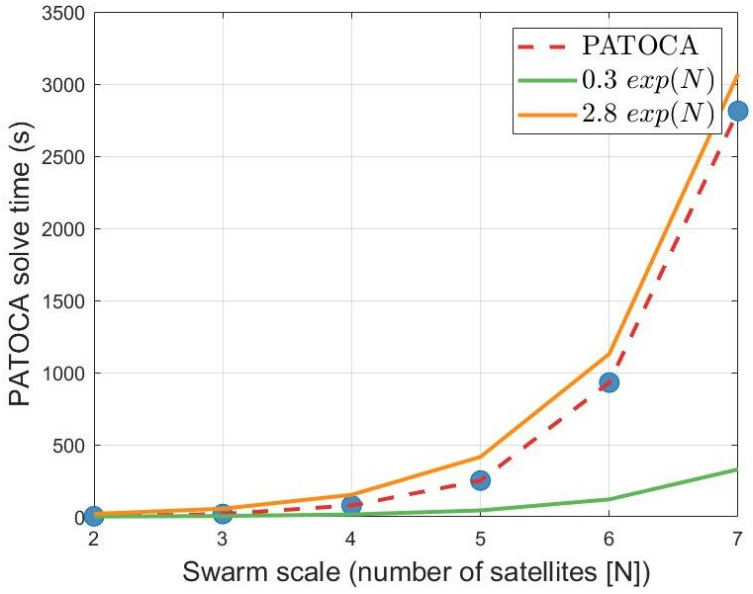

Fig. 4 Computation-time complexity of PATOCA using Gurobi solver

satellites should also respect inter-satellite safety distance R_{safe} to avoid collisions with other neighboring satellites, *i.e.*

$$\textbf{CA constraints: } \|C(\boldsymbol{x}_i(k) - \boldsymbol{x}_j(k))\|_2 \geq R_{\text{safe}}, C = \begin{bmatrix} I_3 & 0_{3\times 1} \end{bmatrix}, \; j \neq i, \; i = 1, 2, \cdots, N, \tag{22}$$

The objective of this TO problem with PA constraints in (21) and CA constraints (22), abbreviated for convenience as PATOCA problem, is to minimize the total fuel consumption by all N satellites over the entire time horizon

$$\min_{u,\boldsymbol{x},\mathcal{B}} J = \sum_{i=1}^{N} \sum_{k=0}^{N_k-1} \sum_{m=1}^{3} |u_{im}(k)|$$

subject to (18) – (21). As noted in [3, 6], since the CA constraints in (22) are in concave form, it cannot be immediately adopted for an efficient computation of satellite trajectories. In the works of [9], authors developed a MILP formulation which yields $O(\exp(N))$ computation-time complexity, as shown in Figure 4 for PATOCA problem, and therefore, such MILP based formulation of CA constraints in the PATOCA problem is not ideal for a large scale formation.

To reduce the computational complexities of the PATOCA problem, we therefore have to decouple the trajectory planning problem into various subcomponents such as (1) PA problem and (2) TO problem. In this work, we present two different approaches to formulate CA constraints and solve trajectory planning problem by augmenting CA constraints with either TO problem, as in [6, 7], or with PA problem. The solution to the trajectory planning problem with both approaches are given in Section VI and VII. Before that, we present here basic PA and TO formulation without CA constraints.

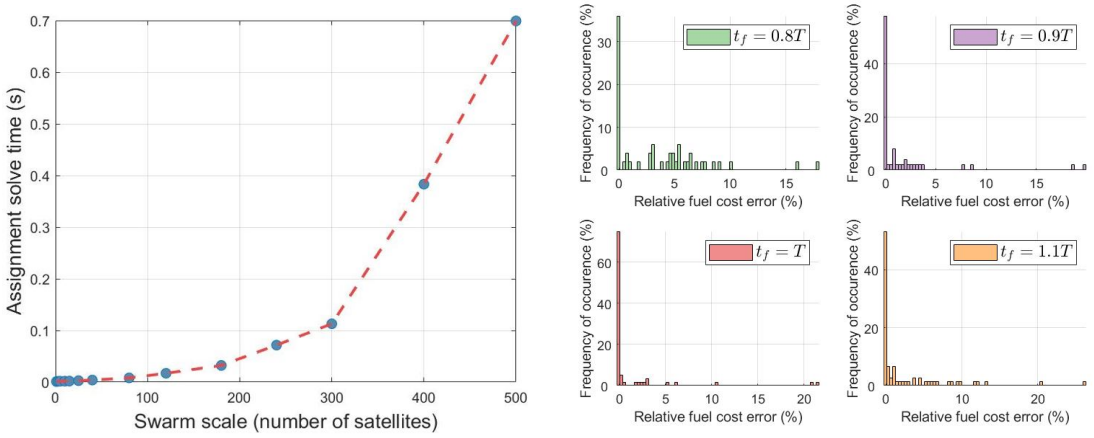

(a) Time complexity of min. distance PA problem using Gurobi solver

(b) Probability distribution of the relative fuel cost error between coupled and decoupled PATO problem for $t_f \in \left[0.8T, 1.1T\right]$ with mean $\mu = 3.5249,\ 1.6992,\ 1.3399,\ 2.45$ and standard deviation $\sigma = 4.08,\ 4.05,\ 4.14,\ 4.83$

Fig. 5 Computation-time complexity of PA and loss of fuel optimality of decoupled PATO relative to coupled PATO problem with minimum-distance PA formulation

A. PA problem formulation:

To solve a PA problem, a distributed auction based assignment was proposed in [24]. As noted in [24], when the dynamics of a robot/satellite is modeled as double integrator systems, PA problem can be formulated as a minimum distance based assignment problem where the distance between the initial and terminal points can be used as an assignment cost. The computational complexity of such PA formulation is shown in Figure 5(a).

Minimum distance formulation allows an efficient computation of final assignment of satellites, as seen from Fig. 5(a). However, oversimplified approximation of the satellite dynamics as a double integrator model, may lead to suboptimal actuation and trajectory prediction. With the help of Monte-Carlo simulations, we evaluate the loss of fuel optimality as the PATO problem is decoupled into minimum distance based PA problem and TO problem. For terminal time $t_f \in [0.8T, 1.1T]$, initial and final positions drawn from two uniform random distributions $\mathcal{U}(-1, 1)$ km and $\mathcal{U}(-5, 5)$ km, the probability distributions of the relative fuel cost error are shown in Figure 5(b). For $t_f = 0.8T,\ 0.9T,\ T,\ 1.1T$, there are respectively 36%, 54.55%, 80% and 53.33% cases where minimum distance assignment is same as the minimum fuel assignment and associated relative fuel cost error is 0%. Clearly, as t_f tends to T, we numerically find that the solution to the decoupled PATO problem is identical with its coupled counterpart for about 80% of cases. On either side of $t_f = T$, frequency of such occurrences decrease gradually. Nevertheless, for different t_f's, there are about 96% cases for which the decoupled fuel cost is at most 10% more than the coupled PATO cost.

However, in practical SFF missions where multiple reconfiguration tasks are performed, it is required that the loss of

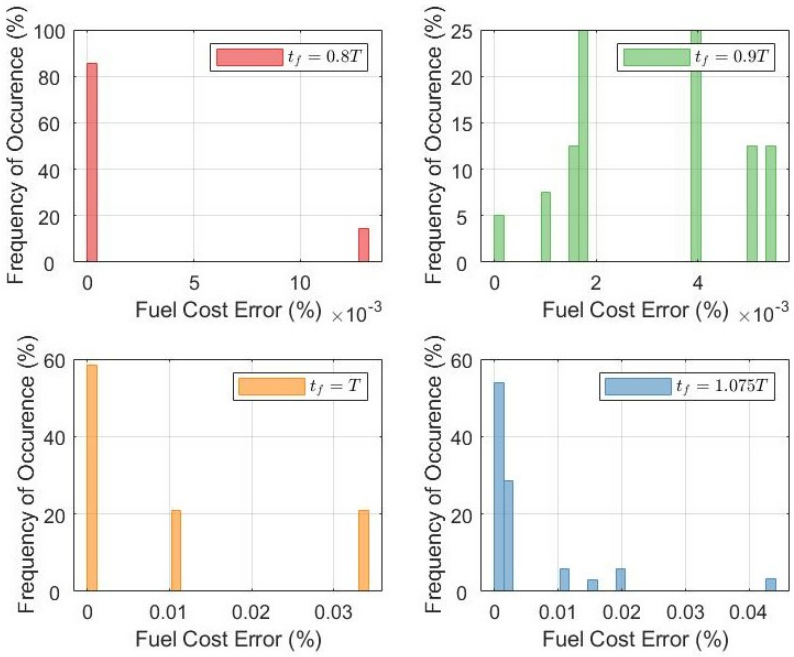

Fig. 6 Probablity distribution (evaluated from 1500 **numerical simulations) of the relative fuel cost error between coupled and decoupled PATO problem under minimum-fuel PA formulation with mean** $\mu = 0.00189,\ 0.0030342,\ 0.009795,\ 0.0040349$**, standard deviation** $\sigma = 0.0046166,\ 0.0017229,\ 0.013162,\ 0.008956$**, swarm size** $\in [1, 20]$**,** $t_f \in [0.8T, 1.1T]$**.**

fuel optimality is kept as small as possible. Inspired by the works of [8], in this work, we formulate an assignment problem where instead of minimizing the overall distance $\sum_{i=1}^{N}\sum_{j=1}^{N} d_{ij}^{\min}$ between initial and target points i and j, we minimize total fuel cost $\sum_{i=1}^{N}\sum_{j=1}^{N} f_{ij} = F\mathcal{B}$. The PA problem can therefore be rewritten as

$$\textbf{PA problem :} \min_{\mathcal{B}} J_P = F\mathcal{B} \text{ subject to PA constraints in (21).}$$

Note that, $F\mathcal{B}$ calculates the fuel cost associated with each configuration, and a centralized coordinator selects a configuration that minimizes the total fuel cost for the swarm. Such formulation allows an efficient computation of satellite assignment, identical to the minimum distance based formulation, while there is no apparent loss of fuel optimality, as seen from a numerical simulation result in Figure 6.

B. TO problem formulation:

In the above PA problem, we need information on fuel cost matrix $F = [f_{ij}]_{N\times N}$ where f_{ij} denotes the fuel cost of satellite i as it moves from location i in initial formation to j in the final formation. Each satellite evaluates the fuel cost to move to each of the final locations in the formation. These simple calculations are done in parallel by each satellite

solving a decentralized TO algroithm which is summarized below.

$$\textbf{TO problem :}\ \min_{u,\boldsymbol{x}} J_T = \sum_{i=1}^{N}\sum_{k=0}^{N_k-1}\sum_{m=1}^{3}|u_{im}(k)| \text{ subject to state space, boundary and control constraints (18), (20).}$$

C. SHMPC to mitigate the effects of modeling uncertainties

In all these discussions, we did not take into account the effects of unmodeled disturbances and modeling uncertainities. If left unaccounted, such disturbances and ignored nonlinear effects will cause large trajectory errors and suboptimal actuation. In this work, we present SHMPC to iteratively mitigate the effects of such uncertainities by evaluating a new control input over a prediction horizon based on the current state information. For a fixed final formation and time, SHMPC successively computes an optimal actuation command which can steer the actual satellite from its current location to its final location at t_f. With the update of new state information, the prediction horizon window shrinks as the start time of the trajectory planning algorithm gradually approaches to t_f. This method of successive prediction and reoptimizing the trajectory planner with more accurate initial positions thus yields a more robust control law that eventually renders a small trajectory prediction error in the face of modeling uncertainities and ignored perturbations.

Algorithm 1: Finding robust control solution to trajectory planning algorithm

Result: Robust control sequence $u_R^*(k),\ k \in [0, t_f]$
Input: $\boldsymbol{x}_S, \boldsymbol{x}_D, u_{\max}, u^r_{\max}, t_f = T, \beta$.
Initialize $\alpha = 0, \boldsymbol{x}(0) = \boldsymbol{x}_S, \boldsymbol{x}(T) = \boldsymbol{x}_D$.
while $\alpha < 1$ **do**
  $[\boldsymbol{x}^*, u_c^*]$ = solution to TO algorithm for the prediction horizon $[\alpha T, T]$.
  Apply u_c^* on the high-fidelity dynamics in (1)-(3) $\dot{\boldsymbol{x}} = f(\boldsymbol{x}, u_c^*)$ with $\boldsymbol{x}(0) = \boldsymbol{x}_S$ in the interval $[\alpha T, (\alpha+\beta)T]$.
  $\boldsymbol{x}_S = \boldsymbol{x}((\alpha+\beta)T)$.
  $u_R^*(k) = u_c^*(k),\ k \in [\alpha T, (\alpha+\beta)T]$.
  $\alpha = \alpha + \beta$.
end
return u_R^*.

In this work, we assume that the high-fidelity nonlinear dynamics in (1) – (3) captures actual satellite motion under J2 perturbation and air drag. Let us take for convenience $t_f = T$ and three positive real numbers $0 < \alpha \leq 1, \beta$. Initially, we assign $\alpha = 0$ and compute an optimal control sequence $u_c^*(k),\ k \in [\alpha T, T]$ from trajectory planning algorithm for the fleet of N spacecraft with initial and terminal state vectors being respectively $\boldsymbol{x}(\alpha T)$ and $\boldsymbol{x}(T)$. Then, by applying the predicted control sequence $u_c^*(k)$ for the interval $k \in [\alpha T, (\alpha+\beta)T]$, we evaluate the actual state measurements of the satellite from (1) – (3) at $(\alpha+\beta)T$. Using the updated state vector $\boldsymbol{x}((\alpha+\beta)T)$ as the initial state vector for the second round of prediction in the interval $[(\alpha+\beta)T, T]$, we determine a new optimal control sequence $u_c^*(k),\ k \in [(\alpha+\beta)T, T]$ which is then applied in open-loop to the actual satellite motion in (1) – (3) to find a new actual state measurement and this procedure is repeated numerous times. More frequent the optimization happens (*i.e.*

smaller the β), lesser is the trajectory prediction error. This algorithm is summarized in Algorithm 1. We now present our main results consisting of two trajectory planning algorithms.

VI. Decoupled Path Assignment (PA) and TO with Collision Avoidance (TOCA): Approach 1

In this section, we present a trajectory planning problem which is decoupled into PA problem and TO Problem. Given a set of N satellites in a concentric PCO, we first determine the fuel optimal final configuration of satellites by solving a PA problem, defined in Section V.A. USing these terminal states as an input, we then solve decentralized TO problem for each satellite with the formulation given in Section V.B. However, as the satellites manuever between initial and target locations, they have to maintain inter-satellite safety distance from one another. In this approach, CA constraints are embedded within TO problem. A TO problem with nonconvex CA constraints are NP complete problems [5] which are computationally difficult. As noted earlier, CA constraints, formulated with MIL constraints in [9] cannot be extended to a large SFF problem either. A heuristic convex approximation of CA constraints was proposed in [26], while an affine CA approximation in [6]. Inspired by the works of [6, 7], CA constraints in (22) are transformed into

$$\textbf{Affine CA constraints:} \quad \left(\bar{\boldsymbol{x}}_i(k)-\bar{\boldsymbol{x}}_j(k)\right)^{\mathrm{T}} C^{\mathrm{T}} C\left(\boldsymbol{x}_i(k)-\boldsymbol{x}_j(k)\right) \geq R_{\text{safe}} \| C\left(\bar{\boldsymbol{x}}_i(k)-\bar{\boldsymbol{x}}_j(k)\right) \|_2, \; j>i, \tag{23}$$

where $\bar{\boldsymbol{x}}_i, \; i=1,2,\cdots,N$ is an initial guess of the optimal trajectory followed by i^{th} spacecraft. The closer the selection of this initial guess to the actual trajectory, the more accurate will be the solution to the resulting convexified TOCA problem. An initial guess is generated by first solving a convex TO problem (without CA constraints) and then this initial guess is passed on as nominal trajectory $\bar{\boldsymbol{x}}_i$ for subsquent iterations of conevexified TOCA algorithm. In iteration $\mathbf{m}$, the solution to the previous iteration is used as a nominal trajectory $\bar{\boldsymbol{x}}_i(k) = \boldsymbol{x}_{i,\mathbf{m}-1}(k)$ for formulating CA constraints in (24). These iterations will continue to give an updated nominal trajectory until it eventually converges to actual collision-free trajectories of each satellite, *i.e.* $\|\boldsymbol{x}_{i,\boldsymbol{m}}(k) - \boldsymbol{x}_{i,\boldsymbol{m}-1}(k)\|_2 < \epsilon, \forall i = 1,2,\cdots,N$. This TOCA problem is solved in a distributed manner where nominal trajectories are communicated by each spacecraft i to other neighboring satellites $\mathcal{N}_i = \{j\}$ with $\|C(\boldsymbol{x}_i(k) - \boldsymbol{x}_j(k))\|_2 \geq R_{\text{comm}}$. The TOCA problem can thus be formulated as follows:

$$\textbf{TOCA problem:} \min_{u,\boldsymbol{x}} J_{TC} = \sum_{i=1}^{N} \sum_{k=0}^{N_k-1} \sum_{m=1}^{3} |u_{im}(k)|$$

subject to state space dynamics with boundary points (18), control constraints (20) and affine CA constraints (24). An SCP method for solving this distributed TOCA algorithm is given in Method 1 of [31]. To robustify this TOCA algorithm against any modeling uncertainities and disturbances, we apply SHMPC in Algorithm 1 repeatedly throughout the reconfiguration task with the "TO" problem in the "WHILE" loop now being replaced with "TOCA problem". The trajectory planning algorithm consisting of a centralized PA problem and distributed TOCA problem is summarized

below in Algorithm 2.

Algorithm 2: Finding robust control solution to guarantee collision-free fuel optimal trajectories-Approach 1

Result: Robust fuel optimal control sequence $u_i^*(k),\ k \in \left[0, t_f\right]$ and collision-free predicted trajectories $\boldsymbol{x}_i^*, i \in \{1, 2, \cdots, N\}$

Input: $\boldsymbol{x}_{iS}, \boldsymbol{x}_{iD}, u_{i,\max}, u_{i,\max}^r, t_f, \beta, R_{\text{safe}}, R_{\text{comm}}, \epsilon$.

f_{ij} := solve decentralized TO problem in Section V.B with $\boldsymbol{x}_i(0) = \boldsymbol{x}_{iS},\ \boldsymbol{x}_i(T) = \boldsymbol{x}_{jD},\ \forall j \in 1, 2, \cdots, N$.

$F := [f_{ij}]_{N\times N}$.

$\mathcal{B}$:= solve centralized PA problem in Section V.A.

$\boldsymbol{x}_{iD} = \mathcal{B}(i, j)\, \boldsymbol{x}_{jD},$ if $\mathcal{B}(i, j) \neq 0$.

$[u_i^*, \boldsymbol{x}_i^*]$:= solve SHMPC in Algorithm 1 with SCP based distributed TOCA formulation, given $\boldsymbol{x}_{iS},\ \boldsymbol{x}_{iD}, R_{\text{safe}}$, $R_{\text{comm}}, \epsilon$, and number of SHMPC prediction windows $\dfrac{t_f}{\beta}$.

return u_i^*.

In contrast with the works of [24] where a distributed auction algorithm was presented to solve the satellite assignment problem, the minimum fuel PA formulation completely relaxes the communication requirement. Furthermore, as noted previously, this centralized PA formulation provides a simple computationally efficient method of finding an optimal assignment of the satellites in the final formation. The reference satellite acts as a centralized coordinator which solves this PA problem and disseminates the solution to all N follower satellites. The results presented here can be extended to other constellation formation flying missions with multiple target orbits and a cluster of satellites around each of them. In that case, reference satellites, defining the target orbits serve as a central processor for each local clusters.

The effectiveness of the proposed trajectory planning algorithm (approach 1) is illustrated now with the help of a numerical example. The reference orbit is an SSO with Keplerian parameters $a = 6800$ km, $e = 0, i = 97^\circ, \Omega = 10^\circ, \theta = 0^\circ$ and the position and velocity vector of this reference satellite evolves according to (5) – (11). The swarm reconfiguration problem requires a group of 10 satellites move from one PCO to another in one orbital period, *i.e.* $t_f = T$ under 3 mN maximum actuation while maintaining inter-satellite safety distance $R_{\text{safe}} = 75$ m and formation center being the reference satellite. Out of 9 follower satellites, a set of 4 satellites move to a PCO with radius 150 m and the other 5 satellites to a PCO with radius 350 m. For this swarm reconfiguration problem, we consider discretization time step to be 10 s.

Given the initial and final locations of 9 follower satellites, we first evaluate the fuel cost matrix F by solving 9 decentralized TO problems in parallel for each satellite. Using this fuel cost matrix F, we then determine the minimum-fuel final assignment of satellites by solving a centralized PA problem, given in Section V.A and the resulting final configuration of satellites is shown in Figure 7(a) where initial (marked in circles) and assigned final location (marked in squares) pairs are marked in same colors. Next, by solving a decentralized TO problem (without considering CA constraints) as in Section V.B, we observe that there are 10 instances where 5 pairs violate the inter-satellite safety distance. By solving the presented TOCA problem with SCP, satellites 5, 7, 8 and 9 find collision-free paths from the feasible space with 1.1%, 1.44%, 0.012% and 8.09% respective loss of fuel optimality. The total number of SCP

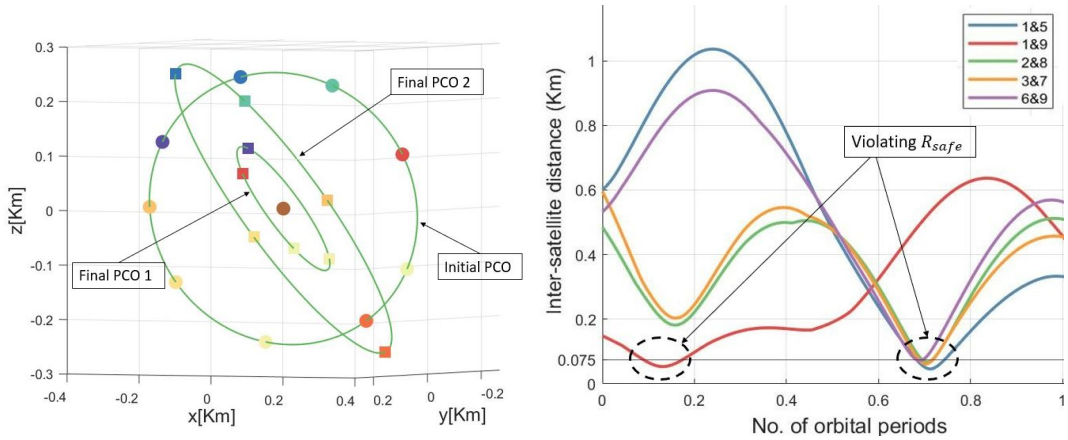

(a) Final assignment of satellites

(b) Inter-satellite distance without TOCA

Fig. 7 Swarm reconfiguration problem of 9 satellites

iterations required for TOCA solution to coverge is 5 and under the TOCA algorithm, these satellites now maintain required R_{safe} distance from one another, as seen from the Figure 8. Furthermore, the effects of unmodeled perturbations are mitigated with our SHMPC in Agorithm 1, the predicted trajectory error which was in the order of few cm in this specific example problem, now improves to a mm precision level. The approximate run-time of this SHMPC-SCP algorithm in Gurobi solver is now in the order of 10 seconds. Therefore, approach 1 efficiently solves the swarm reconfiguration problem. However, solving this TOCA problem requires all the satellites to share their updated state information to its neighboring members at every time steps. This eventually results in a large communication overhead. In case, when a communication link between two neighboring satellites is suddenly broken due to sensor malfunction, this SCP-TOCA formulation will remain misinformed about the presence of a neighbor within a satellite's safety sphere of radius R_{safe} and thus the predicted actuation command by the trajectory planner will not be able to steer the satellite through a collision-free path. To avoid the problems associated with real-time communication while solving this TOCA problem, in this work we present another alternative trajectory planning algorithm for swarm reconfiguration problem in which CA constraints are included within PA optimization problem, discussed next.

VII. Decoupled Path Assignment (PA) with Collision Avoidance (PACA) and TO: Approach 2

In this section, we present a novel trajectory planning approach where we determine collision-free assignment of satellites instead of finding fuel-optimal assignments as in the previous section. The objective of this assignment problem is therefore to find a near optimal final configuration so that the satellites as they steer to the final configuration maintain inter-satellite safety distance all the way. To this end, we include the CA constraints into the PA problem and the resulting optimization problem is termed as PACA.

Similar to the previous approach, we first solve decentralized TO problem in Section V.B to evaluate fuel cost f_{ij}, fuel

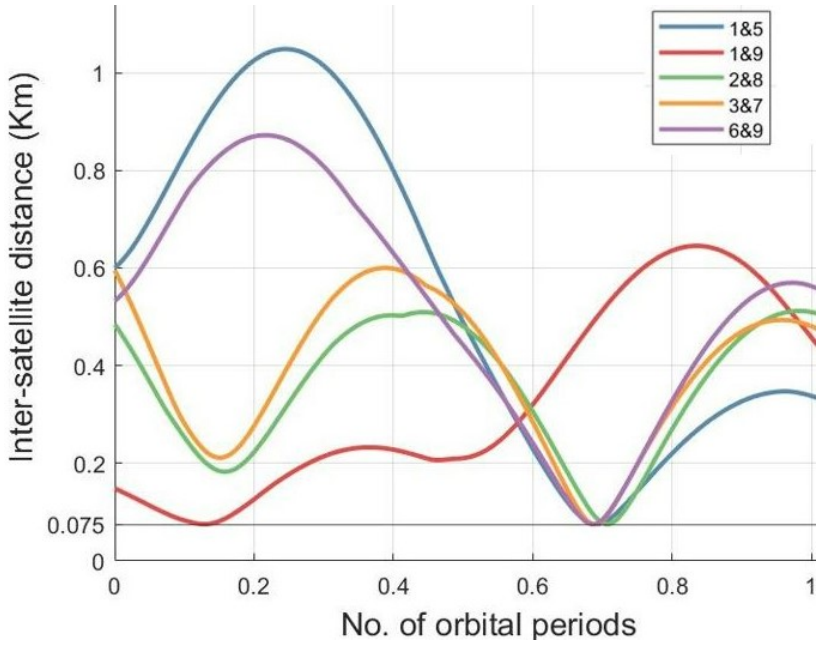

Fig. 8 Inter-satellite distance with TOCA algorithm of approach 1

optimal trajectories $\boldsymbol{x}_{ij}(k)$, actuation $u_{ij}(k)$, $d[i,j,q,p] = \min\left(\boldsymbol{x}_{ij}(k) - \boldsymbol{x}_{qp}(k)\right),\ \forall k \in [0, N_k - 1],\ q > i, j \neq p$ as the satellites i and q occupy the final locations j and p. By using $d[i,j,q,p] > R_{\text{safe}}, \forall i, j$ as the constraints, PACA problem then finds an assignment $i \rightarrow j$ and $q \rightarrow p$, achieving which guarantees collision-free motion of all satellites. The PACA problem can thus be formulated as:

$$\begin{aligned}
&\textbf{PACA problem: } \min_{\mathcal{B}} J_{PC} = \sum_{i=1}^{N}\sum_{j=1}^{N} f_{ij} b_{ij} \text{ subject to } \sum_{i=1}^{N} b_{ij} = \sum_{j=1}^{N} b_{ij} = 1, b_{ij} = \{0,1\},\\
&\textbf{CA constraints: } b_{ij} + b_{qp} \leq 1, \text{ if } d[i,j,q,p] < R_{\text{safe}},
\end{aligned} \tag{24}$$

where CA constraints based on seperating hyperplanes transform the prohibited assignment with suitable affine formulation. However, this PACA problem becomes infeasible if there exists no assignment that satisfies the CA constraints (24). To solve this infeasibility, we include an additional term in the objective function to penalize any large violation from the specified safety margin. The modified PACA problem can thus be rewritten as

$$\begin{aligned}
&\textbf{PACA problem: } \min_{\mathcal{B}, b_c} J_{\mathbf{PC}} = \sum_{i=1}^{N}\sum_{j=1}^{N} f_{ij} b_{ij} + C[i,j,q,p] b_c[i,j,q,p] \text{ subject to } \sum_{i=1}^{N} b_{ij} = \sum_{j=1}^{N} b_{ij} = 1, b_{ij} = \{0,1\},\\
&\textbf{CA constraints: } b_{ij} + b_{qp} \leq 1 + b_c[i,j,q,p], \text{with } b_c[i,j,q,p] \in \{0,1\},
\end{aligned} \tag{25}$$

where $C[i,j,q,p] = R_{\text{safe}} - d[i,j,q,p]$ and $b_c[i,j,q,p]$ is a binary variable that selects an assignment based on minimal violation from R_{safe}. With the resulting assignment $\mathcal{B} = [b_{ij}]_{N\times N}$, we then select satellite trajectories $\boldsymbol{x}_{ij}(k)$

and actuation $u_{ij}(k),\ \forall k$ to be the solution of the trajectory planning problem. Finally, with SHMPC, we robustify the solution to trajectory planning problem against modeling uncertainities, similar to approach 1. The trajectory planning algorithm conisting of centralized PACA and decentralized TO problems is summarized below. In contrast

Algorithm 3: Finding robust control solution to guarantee collision-free near optimal satellite trajectories-Approach 2

Result: Robust fuel optimal control sequence $u_i^*(k),\ k \in \left[0, t_f\right]$ and collision-free predicted trajectories $\boldsymbol{x}_i^*, i \in \{1, 2, \cdots, N\}$

Input: $\boldsymbol{x}_{iS}, \boldsymbol{x}_{iD}, u_{i,\max}, u_{i,\max}^r, t_f, \beta, R_{\text{safe}}$.

$[f_{ij}, \boldsymbol{x}_{ij}]$:= solve decentralized TO problem in Section V.B with $\boldsymbol{x}_i(0) = \boldsymbol{x}_{iS},\ \boldsymbol{x}_i(T) = \boldsymbol{x}_{jD},\ \forall j \in 1, 2, \cdots, N$.

$F := [f_{ij}]_{N\times N},\ d[i,j,q,p] = \min\left(\boldsymbol{x}_{ij}(k) - \boldsymbol{x}_{qp}(k)\right), C[i,j,q,p] = R_{\text{safe}} - d[i,j,q,p]$.

$\mathcal{B}$:= solve centralized PACA problem in Section VII.

$\boldsymbol{x}_{iD} = \mathcal{B}(i,j)\,\boldsymbol{x}_{jD},$ if $\mathcal{B}(i,j) \neq 0$.

$[u_i^*, \boldsymbol{x}_i^*]$:= solve SHMPC in Algorithm 1 on decentralized TO formulation in Section V.B, given $\boldsymbol{x}_{iS},\ \boldsymbol{x}_{iD}$, and number of SHMPC prediction windows $\dfrac{t_f}{\beta}$.

return u_i^*.

with approach 1 where satellites cooperatively determine collison-free paths to reach to fuel optimal assignment, in approach 2 satellites select the trajectories based on collision-free assignment. Doing so, approach 2 relaxes the real-time communication requirement of approach 1 at expense of fuel optimality. The advantages and disadvantages of both approaches are illustrated through a trade-off analysis in Section VIII. To analysze the effectiveness of approach 2, we now consider the same numerical example from Section VI.

A. Illustrative Example

: Consider the same illustrative example as in Section VI. A.

Remark 1 *We talk about artificial potential function based cooperative correction methods to overcome the problems resulting from this formulation.*

VIII. Comparative Analysis of Both Approaches on Performance & Computational Complexity

We present simulation results in this Section to demonstrate the computational complexity with increasing swarm size and compare with other existing approaches in the literature.

IX. Conclusions

Acknowledgments

References

[1] Morgan, D., Chung, S.-J., Blackmore, L., Acikmese, B., Bayard, D., and Hadaegh, F. Y., "Swarm-Keeping Strategies for Spacecraft under J2 and Atmospheric Drag Perturbations," *Journal of Guidance Control and Dynamics*, Vol. 35, No. 5, 2012, pp. 1492–1506.

[2] Krieger, G., Moreira, A., Fiedler, H., Hajnsek, I., Werner, M., Younis, M., and Zink, M., "TanDEM-X: A Satellite Formation for High-Resolution SAR Interferometry," *IEEE Trans. Geosci. Remote Sens.*, Vol. 45, No. 11, 2007, pp. 3317 – 3341.

[3] Lim, H. C., and Bang, H., "Trajectory Planning of Satellite Formation Flying using Nonlinear Programming and Collocation," *J. Astron. Space Sci.*, Vol. 25, No. 4, 2008, pp. 361–374.

[4] Chung, S. J., Bandopadhyay, S., Foust, R., Subramanian, G. P., and Hadaegh, F. Y., "Review of Formation Flying and Constellation Missions Using Nanosatellites," *Journal of Spacecraft and Rockets*, Vol. 53, No. 3, 2016, pp. 1–12.

[5] Garcia, I., and How, J. P., "Trajectory Optimization for Satellite Reconfiguration Maneuvers with Position and Attitude Constraints," *Proceedings of the 2005, American Control Conference, 2005.*, Vol. 2, Portland, USA, 2005, pp. 889–894.

[6] Morgan, D., Chung, S.-J., and Hadaegh, F. Y., "Spacecraft Swarm Guidance Using a Sequence of Decentralized Convex Optimizations," *in Proc. of the AIAA/AAS Astrodynamics Specialist Conference*, Minneapolis, MN, 2012, pp. 1–16.

[7] Morgan, D., Chung, S.-J., and Hadaegh, F. Y., "Decentralized Model Predictive Control of Swarms of Spacecraft Using Sequential Convex Programming," *in Proc. of the AIAA/AAS Astrodynamics Specialist Conference*, Kauai, HI,, 2013, pp. 1–20.

[8] Tillerson, M., Inalhan, G., and How, J. P., "Co-ordination and control of distributed spacecraft systems using convex optimization techniques," *Int. J. Robust Nonlinear Control*, Vol. 12, 2002, pp. 207–242.

[9] Richards, A., Schouwenaars, T., How, J. P., and Feron, E., "Spacecraft Trajectory Planning with Avoidance Constraints Using Mixed-Integer Linear Programming," *Journal of Guidance, Control, and Dynamics*, Vol. 25, No. 4, 2002, pp. 755–764.

[10] Kristiansen, R., and Nicklasson, P. J., "Spacecraft formation flying: A review and new results on state feedback control," *ACTA Astronautica*, Vol. 65, 2009, pp. 1537–1552.

[11] Scharf, D. P., Hadaegh, F. Y., and Ploen, S. R., "A Survey of Spacecraft Formation Flying Guidance and Control (Part I): Guidance," *in Proc. of the American Control Conference*, Denver, Colorado, USA, 2003, pp. 1733–1739.

[12] Rao, A. V., "A Survey of Numerical Methods for Optimal Control," *Advances in the Astronautical Sciences*, Vol. 135, 2010, pp. 497–528.

[13] Lin, X., Shi, X., and Li, S., "Optimal cooperative control for formation flying spacecraft with collision avoidance," *Sci. Prog.*, Vol. 103, No. 1, 2019, pp. 1–19.

[14] Wu, B., Wang, D., and Poh, E., "Energy-optimal low-thrust satellite formation manoeuvre in presence of J 2 perturbation," *Proceedings of the Institution of Mechanical Engineers, Part G: Journal of Aerospace Engineering*, Vol. 225, 2011, pp. 961–968.

[15] Roscoe, C. W. T., Griesbach, J. D., Westphal, J. J., Hawes, D. R., and J. P. Carrico, J., "Force modeling and state propagation for navigation and maneuver planning for CubeSat rendezvous, proximity operations, and docking," *Advances in the Astronautical Sciences*, Vol. 150, 2014, pp. 573–590.

[16] Eshagh, M., and Alamdari, M. N., "Perturbations in orbital elements of a low earth orbiting satellite," *Journal of the Earth & Space Physics.*, Vol. 33, No. 1, 2007, pp. 1–12.

[17] Inalhan, G., and How, J., "Relative dynamics and control of spacecraft formations in eccentric orbits," *Journal of Guidance, Control, and Dynamics*, Vol. 25, No. 1, 2002, pp. 48–59.

[18] Ma, J., "Formation Flying of Spacecrafts for Monitoring and Inspection," Master's thesis, Lulea University of Technology, Sweden, 2009.

[19] Xu, G., and Wang, D., "Nonlinear Dynamic Equations of Satellite Relative Motion Around an Oblate Earth," *Journal of Guidance, Control and Dynamics*, Vol. 31, No. 5, 2008, pp. 1521–1524.

[20] Khalil, I., and Samwel, S., "Effect of Air Drag Force on Low Earth Orbit Satellites during Maximum and Minimum Solar Activity," *Space Research Journal*, Vol. 9, 2016, pp. 1–9.

[21] Schweighart, S., and Sedwick, R., "High-Fidelity Linearized J2 Model for Satellite Formation Flight," *Journal of Guidance, Control, and Dynamics*, Vol. 25, No. 6, 2002, pp. 1073–1080.

[22] Hamel, J.-F., and Lafontaine, J. D., "Linearized Dynamics of Formation Flying Spacecraft on a J2-Perturbed Elliptical Orbit," *Journal of Guidance, Control, and Dynamics*, Vol. 30, No. 6, 2007, pp. 1649–1658.

[23] Wang, D., Wu, B. L., and Poh, E. K., *Satellite Formation Flying*, Intelligent Systems, Control and Automation: Science and Engineering, Vol. 87, Springer, Singapore, 2017.

[24] Morgan, D., Subramanian, G. P., Chung, S. J., and Hadaegh, F. Y., "Swarm assignment and trajectory optimization using variable-swarm, distributed auction assignment and sequential convex programming," *Int. J. Rob. Res.*, Vol. 35, No. 10, 2016, pp. 1261 – 1285.

[25] Slater, G. L., Byram, S. M., and Williams, T. W., "Collision Avoidance for Satellites in Formation Flight," *in Proc. of the AIAA/AAS Astrodynamics Specialist Conference and Exhibit*, AIAA, Providence, RI, 2004, pp. 1 – 17.

[26] Acikmese, B., Scharf, D. P., Murray, E. A., and Hadaegh, F. Y., "A Convex Guidance Algorithm for Formation Reconfiguration," *in Proc. of the AIAA Guidance, Navigation, and Control Conference and Exhibit*, AIAA, Keystone, CO, 2006, pp. 1–17.

[27] Keviczky, T., Borrelli, F., Fregene, K., Godbole, D., and Balas, G. J., "Decentralized Receding Horizon Control and Coordination of Autonomous Vehicle Formations," *IEEE Transactions on Control Systems Technology*, Vol. 16, No. 1, 2008, pp. 19–33. https://doi.org/10.1109/TCST.2007.903066.

[28] Wu, B., Xu, G., and Cao, X., "Relative Dynamics and Control for Satellite Formation: Accommodating J2 Perturbation," *Journal of Aerospace Engineering*, Vol. 29, No. 4, 2016, p. 04016011. https://doi.org/10.1061/(ASCE)AS.1943-5525.0000600.

[29] Directorate, A. F. R. L. S. V., "TechSat 21 factsheet page," https://www.vs.afrl.af.mil/factsheets/TechSat21.html, 2019. Online; accessed 8 September 2021.

[30] Sidi, M., *Spacecraft Dynamics & Control: A Practical Engineering Approach*, Cambridge Aerospace Series, Vol. 7, Cambridge University Press, 2006.

[31] Morgan, D., Chung, S.-J., and F.Y.Hadaegh, "Model Predictive Control of Swarms of Spacecraft Using Sequential Convex Programming," *Journal of Guidance, Control, and Dynamics*, Vol. 37, No. 6, 2014, pp. 1725–1740.